

Improving Earthquake Resistance of Structures by Injection Consolidation of Earth Foundations

Sergey Prostov¹, Evgeniy Shabanov¹, Michail Sokolov¹, and Musa Shabdanov²

¹T.F. Gorbachev Kuzbass State Technical University, Str. Vesennyyaya, 28, Kemerovo, Russian Federation, 650000

²M.M. AdyshevOsh Technological University, 81 N. Isanovstreet, Osh, Kyrgyz Republic

Abstract. Based on the analysis of the results of field experiments, recommendations were developed on increasing the earthquake resistance of soil foundations of buildings and structures at the Krasnobrodsky coal open-pit mine, providing conditions for an uninterrupted and safe technological process of minerals extraction and transportation. As a result of research carried out at a pilot test site by the method of seismic sounding using the refraction technique, scientific and practical results were obtained. It has been experimentally proved that compacting soils with cement-sand mortar allows us to improve their deformation properties, which leads to an increase in the earthquake resistance of structures. The seismicity of the soil foundation of the enrichment complex of inclined separation was calculated on the basis of the performed simulation of deformation processes in the consolidated foundation of the structure in a critical state. The studies have found out that when weakened soils are compacted under the supports of the galleries of the structure and after the artificial foundation has gained strength, seismicity decreased from 7 to 6 points.

1 Introduction

Seismicity in Russia is due to the intense geodynamic interaction of several large lithospheric plates (Pacific, Eurasian, Arabian, African, Indo-Australian, Chinese, Okhotsk and North American) [1-4]. According to the OSR-97 map, which defines seismic zoning and is part of the first global general map of global seismic hazard, the Kemerovo Region refers to areas with moderate seismic activity [5-7].

The most powerful earthquakes with magnitude $M \approx 6$ in the Kemerovo region were noted at the turn of the XIX and XX centuries, no earthquakes with a magnitude of more than 4.5 have been observed since the beginning of the 1960s, but an earthquake of magnitude $M = 5.2$ in the Belovo area on June 19, 2013 drew general attention to the problem of Kuzbass seismic activity [8-10]. Changes in the seismic environment indicate an increase in seismic hazard, seriously underestimated until recently.

In the early 30s of the last century, the intensive development of the Kuzbass coal basin began. The first metallurgical complexes were built, a railway network was extended for large-capacity cargo transportation, and active mining of minerals began using industrial

explosions. With an increase in the volume of extracted rock mass and the scale of blasting in Kuzbass, there was a sharp increase in technogenic seismicity [11]. In the 60s, an increase in the number of technogenic seismic events began, which accelerated sharply after the 80s. Although their power was not large, the number of technogenic seismic events significantly exceeded the number of natural seismic events. Figure 1 shows the total numbers of the largest seismic events (energy class $K > 8.5$), an increase in seismic activity in the period from 1998 to 2005 is noticeable. Judging by the number of earthquakes of grades 9–10, the most powerful was the increase in seismic activity in the period from 2000 to 2005. There were at least 20 earthquakes against 5–6 in the previous two years, but there were only two earthquakes of class 11 in this seismicity rise (no more than in previous rises), and there were no earthquakes of class 12 at all (in 1966 there was one earthquake of class 12).

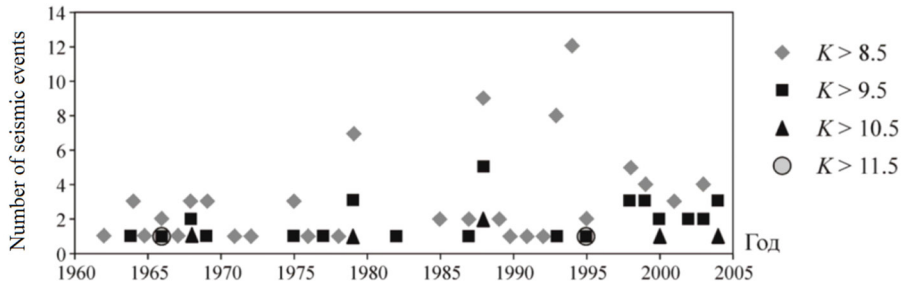


Fig. 1. The annual number of strong seismic events in the period 1962 to 2005 (according to VNIMI).

Until 2000, Kuzbass in terms of seismic zoning mainly belonged to the territory with seismicity basically no more than 6 points, which did not provide for special anti-seismic measures during construction (Fig. 2). According to the standards adopted in the USSR, buildings are designed and constructed as earthquake-resistant in territories with a seismic hazard of 7 points or higher.



Fig. 2. Map of seismic zoning of the Kemerovo region.

Reassessment of the seismic hazard in the region led to an increase in the region seismic magnitude. The use of anti-seismic measures increases the cost of construction of buildings and structures by 30-40%. The situation is complicated by the prevalence of weak flooded soils, in the presence of which seismicity increases by an additional point. The seismic effect on the building at the site with a seismicity of 7 points is 2 times higher than the 6-point seismicity, on 8-point sites this effect is 2 times higher than on 7-point sites, and so on.

Reducing the seismic hazard coefficient is currently an important and relevant socio-economic task. Compaction of soil is one of the ways to achieve this task.

2 Method of research

NOOSTROY LLC conducted an experimental injection compaction of soils at the site of the planned construction of a building in Kemerovo with dimensions of 28x8 m. The foundation was consolidated by pressure injection of cement-sand mortar, which provides for partial hydraulic fracturing of the soil at the initial stage of injection [12]. The consolidation technology is described in detail in the article [13-14]. The soil is represented by brown stiff loam with sandy loam lenses and a bulk mass of 1.7 g/cm³. The initial maximum measured seismic intensity was 7 points, the velocity of transverse (S) waves in the 30-meter thickness varied in the range from 177 to 235 m/s.

To clarify the seismic intensity at the site of injection compaction of soils, the seismic properties of soils were studied [15] at a specially organized testing ground immediately after compaction (in 2 days) and in the process of soil consolidation in 51 day after the compaction.

To calculate the increment of seismic intensity by the method of seismic stiffness, a set of works on seismic sounding by the method of refracted waves (MPW) was performed. The sounding was carried out by Laccolit X-M3 seismic station with 12 channels. The snapping of points on the ground was carried out using the plan (M 1 : 500). The location of seismic sensing points is shown in Fig. 3.

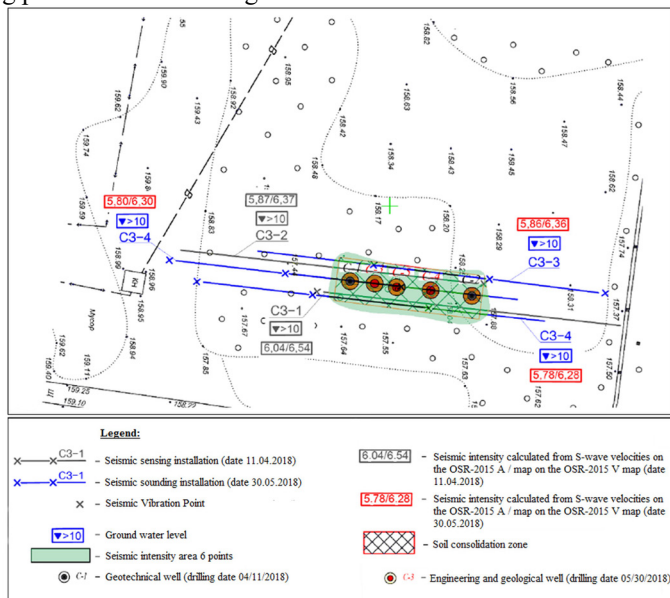


Fig. 3. Map of the test site combined with a map of seismic zoning.

To excite seismic vibrations, a sledgehammer (tamper) weighing 6 kg was used. When recording transverse waves, a strike was applied horizontally in two opposite directions, perpendicular to the line of arrangement of the geophones. To record the transverse waves, horizontal seismic receivers GS20-DX-2B were used. Seismic sounding was carried out in 2 stages: on April 11, 2018 (in 2 days after compaction of the soil, seismic sounding was completed in 2 points), on May 30, 2018 (in 51 day after compaction, seismic sounding was completed in 3 points). The data obtained by the results of seismic sounding were processed in the ZondST2D program. The seismograms obtained from the excitation points PV-1, PV-2, and PV-3 were summarized.

3 Results and Discussion

From the hodographs obtained from the seismograms, the average and boundary velocity of elastic waves were determined. Then the weighted average speed was determined in a 30-meter thickness using the following formula:

$$V_s = \frac{H}{\sum_{i=1}^n t_i} \quad (1)$$

where H – design thickness, m (30 m); t_i – the vertical travel time of the elastic wave in the i -th layer, s;

$$t_i = \frac{h_i}{V_{si}} \quad (2)$$

h_i – thickness of the i -th layer, m; V_{si} – layer velocity in the i -th layer.

A quantitative assessment of the increment of seismic intensity by the method of seismic stiffness was determined by the formula:

$$\Delta I = \Delta I_c + \Delta I_B + \Delta I_{p3}, \quad (3)$$

where ΔI – total increment of seismic intensity (in points) relative to the initial point; ΔI_c - increment of seismic intensity due to differences in soil conditions determined by the formula:

$$\Delta I_c = 1,67 \lg \left(\frac{V_{s3} \cdot \rho_3}{V_{s1} \cdot \rho_1} \right), \quad (4)$$

where V_{s3} , V_{s1} – weighted average values of transversal wave propagation velocities in the reference and studied sections; ρ_3 , ρ_1 – weighted average values of soil densities in the reference and studied areas; ΔI_B – increment of seismic intensity per groundwater level.

$$\Delta I_B = k \cdot e^{-0,04h^2}, \quad (5)$$

where k – coefficient depending on soil conditions, taken equal to 0.5 with density $\rho_3=1,7$ since the studied site is composed of category II soils by seismic properties; h – groundwater level position, m. Figure 4 shows a seismogram characteristic in appearance, and Figure 5 shows results of measurements of seismic intensity. An example of the obtained results of seismic sounding is presented in Figure 5.

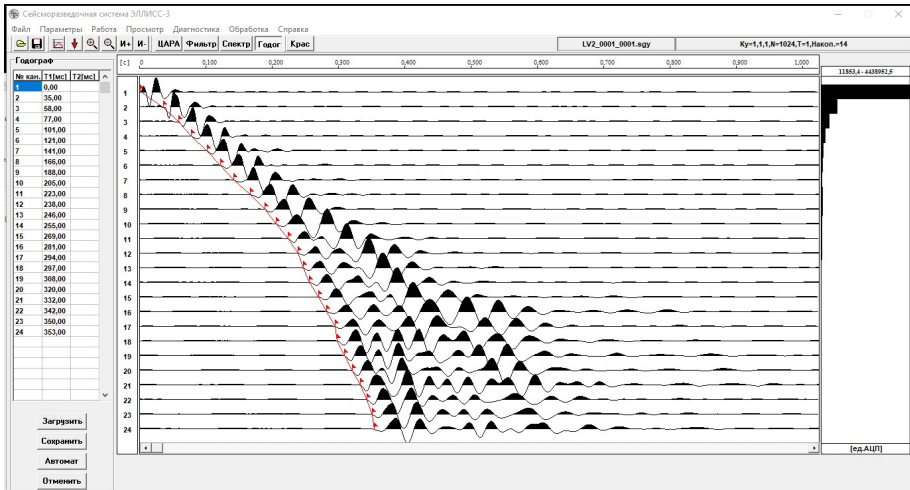


Fig. 4. Seismogram of transverse waves for the first sounding point C3-1.

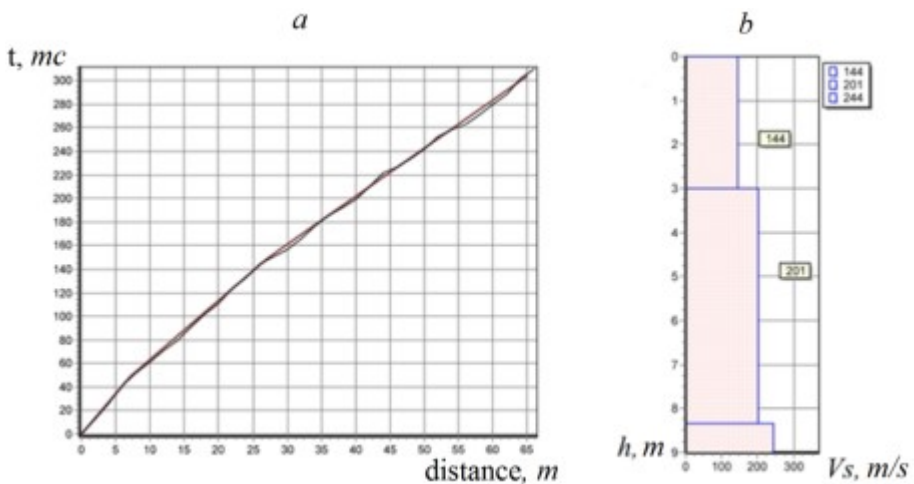


Fig. 5. The results of measurements of seismic intensity in a 30-meter thick soil for point C3-5; hodographs for diving (a); layer velocity model (b).

The weighted average velocity of transverse (S) waves in the 30-meter thickness varies in the range from 220 to 234 m / s at the end of the study (51 day after soil compaction) (Table 1).

Table 1. Calculation of seismic intensity in a 30-meter thick soil.

| Point number C3 | Well number | Weighted average volumetric weight ρ , g/sm ³ | Weighted average transversal wave velocity in a 30-meter thickness | Groundwater Level (UGV), m | Soil dependent coefficient | The increment of seismic intensity I, calculated from the transverse waves, point | Seismic increment, point | Total increment of seismic intensity, point | Site average increment calculated from transversal waves |
|--|-------------|---|--|----------------------------|----------------------------|---|--------------------------|---|--|
| On 11.04.2018 (2 days after soil compaction) | | | | | | | | | |
| C3-1 | C-1 | 1.89 | 161 | > 10 | 1 | 0.24 | 0.00 | 0.24 | 0.16 |
| C3-2 | C-2 | 1.88 | 204 | > 10 | 1 | 0.07 | 0.00 | 0.07 | |
| On 30.05.2018 (51 day after injection) | | | | | | | | | |
| C3-3 | C-3 | 1.92 | 234 | > 10 | 0.5 | 0.06 | 0.00 | 0.06 | 0.01 |
| C3-4 | C-4 | 1.92 | 229 | > 10 | 0.5 | -0.02 | 0.00 | -0.02 | |
| C3-5 | C-5 | 1.92 | 220 | > 10 | 0.5 | 0.00 | 0.00 | 0.00 | |

On April 11, 2018 (2 days after soil compaction), the maximum measured seismic intensity by transversal wave velocities was 6 points (6.04 measured). As of May 30, 2018 (51 day after soil compaction), the maximum measured seismic intensity by transversal wave velocities was 6 points (5.86 measured).

An example of the use of NI is a seasonal concentrator with separators and an inclined separation complex (SPS) in the Krasnobrodsky open-pit coal mine, Branch of OJSC Kuzbassrazrezugol (Figure 2.10).

According to visual surveys and engineering-geological surveys conducted by LLC "NOOCENTER", the structure is in an emergency condition, the pump station has significant uneven subsidence of the supports of conveyor galleries. According to the OSR-2015 seismic zoning maps, the seismicity of the region is 7 points.

The soil is represented by a mixture of landwaste, gravel, blocks, sandy loam and sandy material. The debris and fine aggregate are presented by sedimentary rock of the type of weathered sandstone of low strength.

As a result of a full range surveys, decompression zones were identified and outlined. Prediction of the stress-strain state of the soil foundations of structures was carried out by mathematical modeling using the finite element method and modern geotechnical software systems.

As a result of the simulation, we obtained graphs of the distribution of vertical displacements Δh of the gallery supports from the relative coordinate along the axis of the object (Fig. 6). The main properties of the model are presented in Table 2.

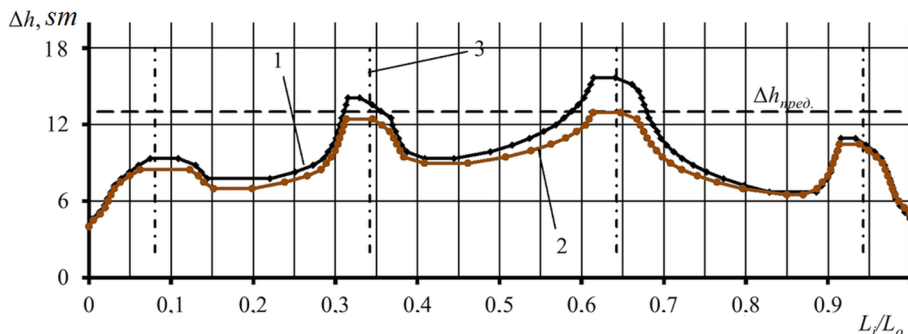


Fig. 6. Distribution of vertical subsidence Δh along the axis: 1 - with a natural base; 2 - when consolidated; 3 - axis of the foundation.

To solve the problem of increasing the stability of the structure, the plan and schemes for soil consolidation by pressure injection were developed (Fig. 2.13).

Table 2. Physical and mechanical properties of model elements.

| Element name | Density ρ , kg/m ³ | Deformation modulus E, MPa | Poisson's ratio ν , D. E. |
|-----------------------|------------------------------------|----------------------------|-------------------------------|
| Soil base | 2050 | 38.0 | 0.29 |
| Decompression area #1 | 1900 | 17.0 | 0.36 |
| Decompression area #2 | 1800 | 12.5 | 0.37 |

The results of the analysis of the distribution of vertical stresses and deformation are presented in Fig. 7. From the obtained dependency graphs, it follows that within the zones of deformation consolidation, ϵ_z is much lower than in a natural massif.

The propagation velocity of longitudinal waves is determined by the formula:

$$V_P = \sqrt{\frac{E \cdot (1 - \nu)}{\rho \cdot (1 + \nu)(1 - 2 \cdot \nu)}}$$

where E – Young's modulus, MPa; ν – Poisson's ratio, D.E.; ρ – density, kg/m³.

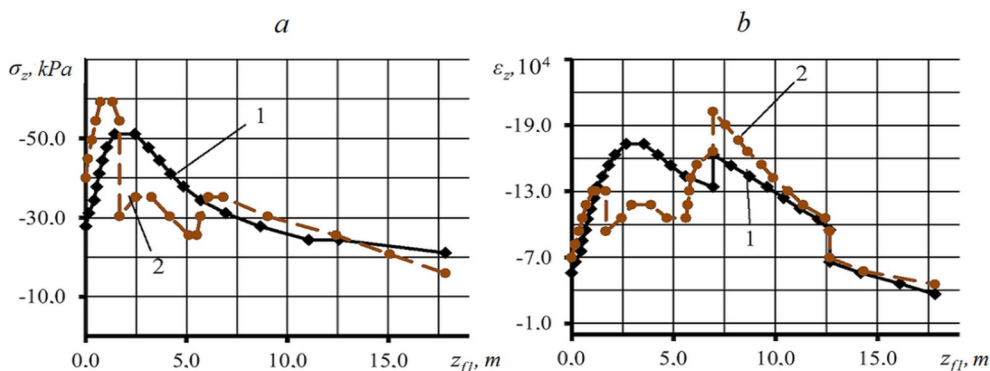


Fig.7. Dependences of the vertical stresses σ_z (a) and the strains ϵ_z (b) on the depth z : 1 - natural massif; 2 - consolidated array.

As a result of injection consolidation, the density of the consolidated areas increases by 10-20%, the Poisson's ratio increases by 10-15%.

The calculated increment of seismic intensity over the longitudinal wave velocities of the natural array ΔI of the first and second decompression areas was 1.1 and 1.2 points, respectively, the increment of seismic intensity ΔI of the simulated consolidated array in the first and second decompression areas is 0.87 and 0.82 points, respectively (tab. 3). The increment of seismic intensity decreased on average by 30%, the seismicity of the soil base decreased from 8.2 to 7.87 points.

As a result of computer modeling and analysis of the results, the effectiveness of the use of pressure injection methods to increase the seismic resistance of the soil of the foundations of structures was established.

Table 3. Calculation of increment of seismic intensity.

| Item name | Density ρ , kg/m ³ | Longitudinal wave velocity V_p , m/s | Deformation modulus E, MPa | Poisson's ratio ν , D.E. | The increment of seismic intensity I, calculated from the longitudinal waves, point |
|--------------------------|---------------------------------------|---|----------------------------------|---------------------------------|---|
| Before consolidation | | | | | |
| Decompression area #1 | 1900 | 122.63 | 17.0 | 0.36 | 1.09 |
| Decompression area #2 | 1800 | 110.83 | 12.5 | 0.37 | 1.20 |
| After consolidation | | | | | |
| Decompression area #1 | 2090 | 150.63 | 20.4 | 0.41 | 0.87 |
| Decompression area #2 | 1980 | 132.71 | 15.0 | 0.41 | 0.82 |

4 Conclusion

According to the results of the study, it was found that on the site with compacted soils, the seismic area moved to a 6-point. At this site, the average increment of seismic intensity decreased from 0.16 to 0.01 points.

From which we can conclude that the consolidation of soils with cement-sand mortar is a very effective method of increasing the seismic resistance of structures, and this conclusion is experimentally proven.

References

1. K. G. Mackey, K. Fujita, H. E. Hartse, *Seismological Research Letters*, **81**, 5, 761 (2010)
2. I. B. Movchan, A. A. Yakovleva, *Journal of Mining Institute*, **236**, 133 (2019)
3. V. V. Adushkin, *Izvestiya. Physics of the Solid Earth*, **49**, 2, 258 (2013)
4. D. V. Rundkvist, Y. G. Gatinsky, W. A. Bush, V. G. Kossobokov, *Computational Seismology and Geodynamics*, **32**, 224 (2013)
5. A. S. Kostinsky, *Modern Science*, **2**, 263 (2017)
6. V. V. Adushkin, *Russian Geology and Geophysics*, **59**, 571 (2018)

7. A. F. Emanov, A. A. Emanov, E. V. Leskova, A. V. Fateev, Geophysical Research Abstracts, **12**, 6657 (2010)
8. A. F. Emanov, A. A. Emanov, A. V. Fateev, E. V. Leskova, E. V. Shevkunova, V. G. Podkorytova, Journal of Mining Science, **50**, 2, 224 (2014)
9. D. V. Yakovlev, T. I. Lazarevich, S. V. Tsirel', Journal of Mining Science, **49**, 6, 862 (2013)
10. V. P. Potapov, O. L. Giniyatullina, I. E. Kharlampenkov, V. N. Oparin, Journal of Mining Science, **51**, 5, 1041 (2015)
11. A. S. Kostinsky, A. P. Gospodarikov, Y. N. Vykhodtsev, M. A. Zatsepin, Journal of Mining Institute, **226**, 405 (2017)
12. E. A. Shabanov, S. M. Prostov, Proceedings of the 8th Russian-Chinese Symposium "Coal in the 21st Century: Mining, Processing, Safety", **92**, 175 (2016)
13. M. V. Sokolov, S. M. Prostov, V. S. Zykov, E3S Web of Conferences, **21**, 01015 (2017)
14. M. Sokolov, S. Prostov, I. Kharitonov, E3S Web of Conferences, **41**, 01016 (2018)
15. A. P. Gospodarikov, K. V. Morozov, I. E. Revin, MIAB. Mining Inf. Anal. Bull., **8**, 157168 (2019)